Backscattering of Gamma Rays from Tin Slabs

By

Masatsugu NISHI*, Takashi NAKAMURA** and Tomonori HYODO**

(Received June 27, 1967)

The backscattering of gamma rays from tin slabs was investigated as a function of slab thickness. The point isotropic ^{60}Co and ^{137}Cs sources were placed on the front face of the scatterer. The obtained data was converted to the response-corrected spectra with the aid of an inverse response matrix, and the angular and energy distributions of backscattered photons were obtained and compared with the other experimental and calculated results.

1. Introduction

A series of measurements of gamma rays backscattered from various material slabs have been carried out using the point isotropic ^{60}Co and ^{137}Cs sources[1-5].

In this paper, the measurements of the backscattered photons from tin slabs as a function of slab thickness are described. This study has two purposes; one is to obtain some information on the backscattering of gamma rays from tin slabs and the other is to compare them with the results for a very large NaI(Tl) crystal in the previous experiment[4], as the effective atomic number of NaI is close to that of tin.

No papers have been published on the variation of backscattered photons with the thickness of tin slabs. A preceeding paper[2] deals with backscattering of gamma rays from tin slabs considered semi-infinite in thickness. In the present work, the angular distributions and the energy spectra of backscattered photons, the number and energy albedos were given as a function of the thickness of tin slabs. These quantities were compared with that for the NaI(Tl) crystal and the calculated values[6-7].

2. Experimental Arrangement and Procedure

Figure 1 shows the geometrical arrangement in this experiment. The scatterer was supported on a rotating table with the axis of rotation on the front face of the scatterer. The scintillation detector head with lead shield was placed on a stand.

* Institute for Chemical Research, Kyoto University
** Department of Nuclear Engineering

The source was placed on the point of intersection of the detector axis and the rotating axis. The distance between the source and the front face of the detector was 80 cm. Nine sets of data were obtained at 10° intervals of the angle θ, which was the angle between the normal to the front face of the scatterer and the detector axis, from 0 to 80°, and one at 85°.

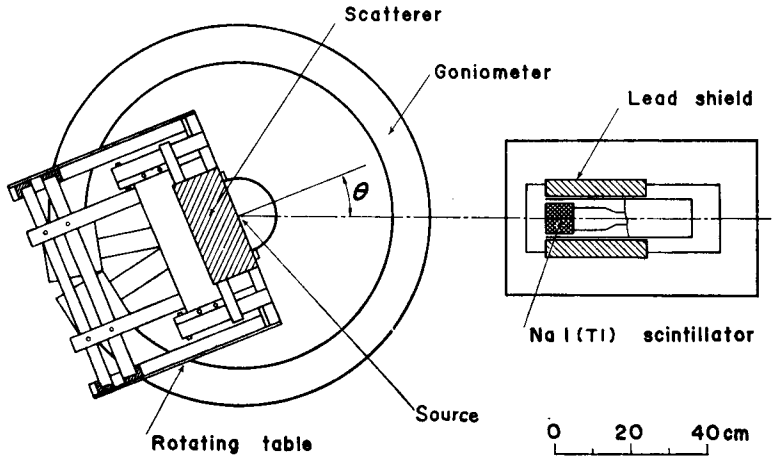

Fig. 1. Experimental arrangement.

The gamma sources were ^{60}Co and ^{137}Cs, prepared by evaporating drops of a solution of high specific activity on very thin mica plates, $\sim$10 mg/cm^2, and covering them with Scotch tape. Their intensities were about 80 μCi and 50 μCi, respectively.

The tin slabs used in this experiment were alloys of 7.277 g/cm^3 density consisting of tin of 97.1 %, antimony of 2.52 %, lead of 0.03 %, and iron of 0.01 % at weight percent which were easily obtained. Thirty sheets of slabs, 2.23 mm thick by 300×300 mm^2 in area, and six sheets of slabs, 1.12 mm thick by 300×300 mm^2 in area, were used as a tin scatterer. The atomic numbers of tin and antimony are 50 and 51, respectively and the atomic number of these slabs is nearly equal to 50.

Previous works[1-2] with a tin scatterer showed that the greater part of back-scattered gamma rays emerges from within a radius of 9 cm from a point source. Therefore, the tin slabs used in this experiment may be regarded as infinitely wide slabs.

The scintillation head consisted of a 3-in. diameter by 3-in. long NaI(Tl) scintillator together with a photomultiplier tube type 6363 and a cathode follower mounted in a single unit. The output pulses of the scintillation head were amplified

by a linear amplifier and fed to a 400-channel pulse height analyzer.

The measured pulse height distributions were converted to the response-corrected spectra with the aid of an inverse response matrix with the energy range 0 to 1.440 MeV[8]. The pulse height distribution was divided into twenty 72-KeV intervals, as in the case of the pulse height interval of the response function matrix, and was designated as P_i. The response-corrected spectrum N_j was obtained* from the product of P_i and M_{ij}^{-1} as

$$N_j = \sum_{i=1}^{20} P_i M_{ij}^{-1}$$

where M_{ij}^{-1} is the (i, j)-element of the inverse response matrix.

3. Results and Discussion

The spectra of backscattered gamma rays were obtained by subtraction of the response-corrected spectra without scatterer from those with scatterer. Before subtraction both spectra had been normalized to a unit solid angle and one primary photon incident on the scatterer. Thus the energy-angle distribution of scattered gamma rays for each slab thickness $N(E, \theta, x)$, was obtained, where E is the photon energy, θ is the emerging angle and x is the slab thickness. The fraction of photons emerging at the angle θ per steradian for one primary photon incident to the scatterer, i.e. the differential number albedo $\alpha(\theta, x)$, and that of energy, i.e. the differential energy albedo $\alpha_E(\theta, x)$, were obtained in the following formulas:

$$\alpha(\theta, x) = \sum_{i=2}^{m} N(E_i, \theta, x) \tag{1}$$

$$\alpha_E(\theta, x) = \sum_{i=2}^{m} N(E_i, \theta, x) E_i/E_0 \tag{2}$$

where E_i is the medium energy of the interval and $m=15$ for ^{60}Co gamma rays ($E_0=1.25$ MeV) and $m=8$ for ^{137}Cs gamma rays ($E_0=0.662$ MeV); the first interval was omitted from the calculation because of the inaccuracy of the input data of this interval. They are shown in Figures 2 and 3 with the emergent angle θ as a parameter.

They are described by

$$\alpha(\theta, x) - b = \{\alpha(\theta, \infty) - b\}(1 - e^{-cx}) \tag{3}$$

$$\alpha_E(\theta, x) - b = \{\alpha_E(\theta, \infty) - b\}(1 - e^{-cx}) \tag{4}$$

excluding the case of the emerging angle $\theta \geq 80°$ for ^{137}Cs gamma rays, where b

* The calculation was carried out by KDC-II computer.

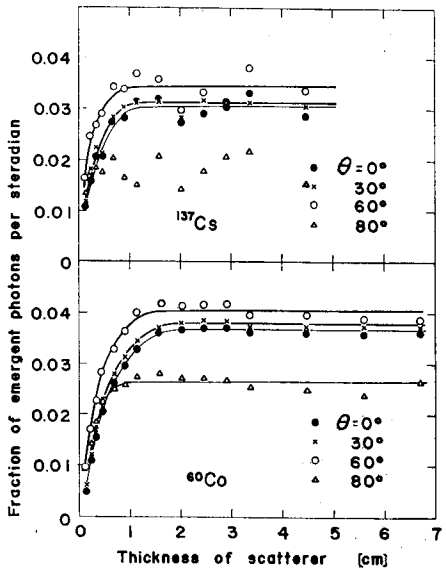

Fig. 2. Differential number albedo $\alpha(\theta, x)$, as functions of emerging angle θ and slab thickness x.

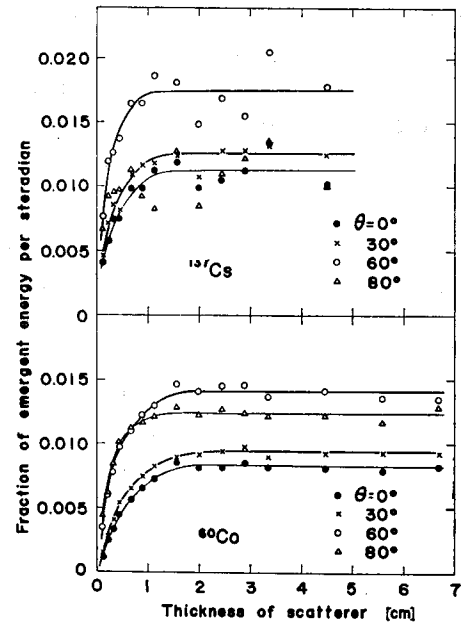

Fig. 3. Differential energy albedo $\alpha_E(\theta, x)$, as functions of emerging angle θ and slab thickness x.

Table I. Asymptotic values of $\alpha(\theta, \infty)$ and $\alpha_E(\theta, \infty)$ and values of b and c*.

Source	Emerging angle, θ (degree)	Number		
		$\alpha(\theta, \infty)$	b	c (cm)$^{-1}$
^{60}Co	0	0.0368±0.0002	−0.0033±0.0007	2.02±0.06
	30	0.0379±0.0002	−0.0028±0.0006	2.13±0.06
	60	0.0404±0.0003	−0.002 ±0.001	2.7 ±0.1
^{137}Cs	0	0.0304±0.0004	0.003 ±0.002	2.9 ±0.3
	30	0.0310±0.0004	0.004 ±0.002	3.1 ±0.3
	60	0.0342±0.0006	0.005 ±0.004	4.5 ±0.8
Source	Emerging angle, θ (degree)	Energy		
		$\alpha_E(\theta, \infty)$	b	c (cm)$^{-1}$
^{60}Co	0	0.00835±0.00007	−0.0006±0.0002	1.88±0.09
	30	0.00944±0.00005	−0.0003±0.0002	1.86±0.06
	60	0.0141 ±0.0001	0.0002±0.0005	2.4 ±0.1
^{137}Cs	0	0.0112 ±0.0003	0.002 ±0.001	2.6 ±0.5
	30	0.0125 ±0.0002	0.0024±0.0008	2.5 ±0.3
	60	0.0174 ±0.0004	0.003 ±0.002	3.5 ±0.8

* The errors are the probable errors by the method of least squares. See text.

and c are constants, and $\alpha(\theta, \infty)$ and $\alpha_E(\theta, \infty)$ are asymptotic values of $\alpha(\theta, x)$ and $\alpha_E(\theta, x)$, respectively. The values of $\alpha(\theta, \infty)$, $\alpha_E(\theta, \infty)$, b and c are shown in Table I. The values of b are pretty small compared with the values of $\alpha(\theta, x)$ and $\alpha_E(\theta, x)$, and may be regarded as zero. Then Equations (3) and (4) have the same form obtained by Bulatov and Garusov[9] for collimated incident gamma rays.

The differential number albedo, $\alpha(\theta, x)$, and the differential energy albedo, $\alpha_E(\theta, x)$, are also shown in Figs. 4 and 5 with the slab thickness x as a parameter, together with their asymptotic values, $\alpha(\theta, \infty)$ and $\alpha_E(\theta, \infty)$, respectively. Comparing $\alpha(\theta, \infty)$ and $\alpha_E(\theta, \infty)$ with the ones calculated by the Monte Carlo method[6] (a semi-infinite medium, 1-MeV and 0.5-MeV incident energies) which are drawn on the dotted lines in Figs. 4 and 5, the agreement between experimental results and calculations is fairly good, in spite of the little difference of the incident energy (0.662 MeV vs. 0.5 MeV, 1.25 MeV vs. 1.0 MeV).

The number albedo, $\alpha(x)$, the energy albedo, $\alpha_E(x)$, and the energy spectrum $N(E, x)$ were calculated using the following formulas:

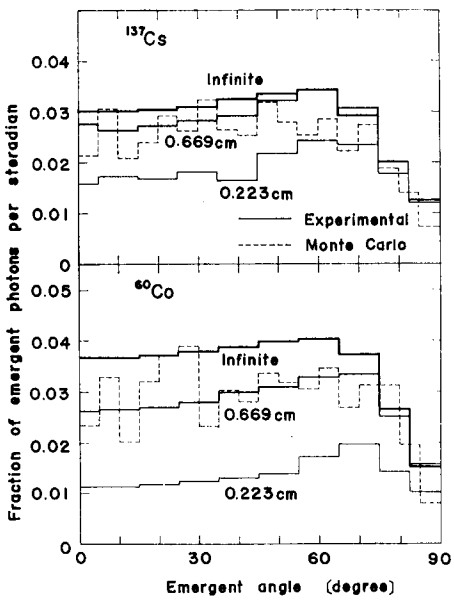

Fig. 4. Angular distribution of backscattered photons as a function of slab thickness. Asymptotic values $\alpha(\theta, \infty)$ and Monte Carlo values for 1.0-MeV and 0.5-MeV gamma rays for semi-infinite tin scatterer obtained by Berger and Raso[6] are also shown.

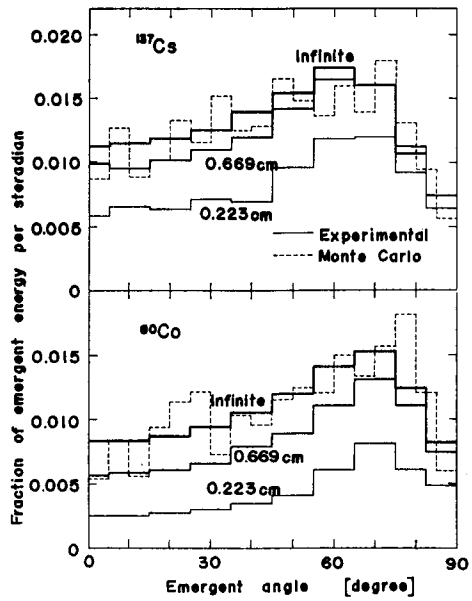

Fig. 5. Angular distribution of backscattered energies as a function of slab thickness. Asymptotic values $\alpha_E(\theta, \infty)$ and Monte Carlo values[6] are also shown.

$$\alpha(x) = \sum_{k=0}^{9} \alpha(\theta_k, x)\, \Omega_k \tag{5}$$

$$\alpha_E(x) = \sum_{k=0}^{9} \alpha_E(\theta_k, x)\, \Omega_k \tag{6}$$

$$N(E, x) = \sum_{k=0}^{9} N(E, \theta_k, x)\, \Omega_k \tag{7}$$

where

$$\begin{aligned}
\Omega_k &= \int_0^{\Delta\theta/2} 2\pi \sin\theta d\theta && \text{for } k=0 \\
&= \int_{(k-(1/2))\Delta\theta}^{(k+(1/2))\Delta\theta} 2\pi \sin\theta d\theta && \text{for } 1 \leq k \leq 7 \\
&= \int_{(8-(1/2))\Delta\theta}^{(8+(1/4))\Delta\theta} 2\pi \sin\theta d\theta && \text{for } k=8 \\
&= \int_{(9-(3/4))\Delta\theta}^{9\Delta\theta} 2\pi \sin\theta d\theta && \text{for } k=9
\end{aligned}$$

The number and energy albedos increase with increasing slab thickness as shown in Figure 6, and approach saturated values when the slab thickness is about one mean free path, where the mean free path of tin is about 2.67 cm for 1.25 MeV gamma rays. As the mean free path of NaI is about 5.2 cm for 1.25-MeV gamma rays and the NaI(Tl) crystal used in the previous experiment[4] was 12.5 cm thick, this experimental result shows that the NaI(Tl) crystal may be considered semi-infinite.

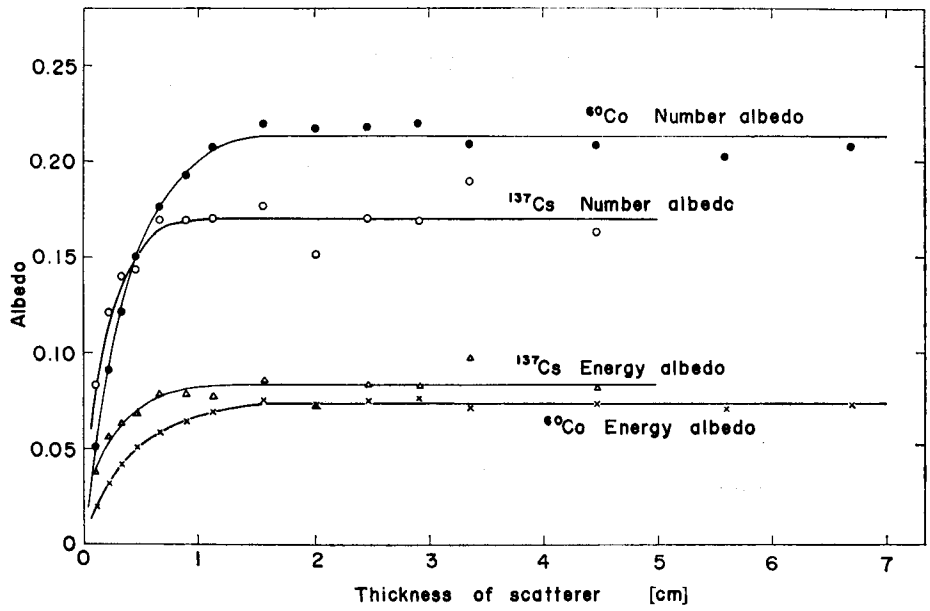

Fig. 6. Number and energy albedos, $\alpha(x)$ and $\alpha_E(x)$, as a function of slab thickness.

Previous work[3] showed that the following formulas hold:

$$\alpha(x)-b = \{\alpha(\infty)-b\}(1-e^{-cx}) \quad (8)$$

$$\alpha_E(x)-b = \{\alpha_E(\infty)-b\}(1-e^{-cx}) \quad (9)$$

Table II shows the values of $\alpha(\infty)$, $\alpha_E(\infty)$, b and c, where $\alpha(\infty)$ and $\alpha_E(\infty)$ are asymptotic values of $\alpha(x)$ and $\alpha_E(x)$, b and c are constants. For tin, the values of b are rather small compared with the values of $\alpha(\infty)$ and $\alpha_E(\infty)$, and may be regarded as zero especially for ^{60}Co gamma rays.

Table II. Asymptotic values of albedos and values of b and c*.

Source	Type	Albedo	c (cm)$^{-1}$	b
^{60}Co	Number	0.214 ±0.001	2.8±0.1	−0.011±0.007
	Energy	0.0735±0.0004	2.5±0.1	0.002±0.002
^{137}Cs	Number	0.170 ±0.002	4.5±0.7	0.03 ±0.02
	Energy	0.083 ±0.002	3.4±0.7	0.020±0.009

* The errors are the probable errors by the method of least squares. See text.

Table III. Albedos*.

Worker \ Source / Scatterer		^{60}Co Number albedo	^{60}Co Energy albedo	^{137}Cs Number albedo	^{137}Cs Energy albedo
This work (experimental)	Tin	0.21 ±0.01	0.074 ±0.004	0.17 ±0.02	0.083 ±0.02
Berger and Raso[6] (Monte Carlo)	Tin	0.17	0.070	0.16	0.085
Shimizu and Mizuta[7] (invariant imbedding)	Tin	——	0.068	——	0.085
Nakamura and Hyodo[4] (experimental)	NaI	0.21 ±0.01	0.073 ±0.004	0.15 ±0.02	0.076 ±0.02

* The errors are ten times the probable errors. See text.

In Table III, the experimental values of the number and energy albedos, $\alpha(\infty)$ and $\alpha_E(\infty)$, are compared with the results of Monte Carlo calculation[10] and of the calculation by the invariant imbedding method[7]. Our experimental values show very good agreement with the calculated ones. Table III also includes the experimental values[4] of the number and energy albedos for NaI(Tl). The experimental values for NaI(Tl) show very good agreement with the experimental and calculated values for tin. This would mean that the idea of the effective atomic number suggested by Berger and Raso[6] is correct.

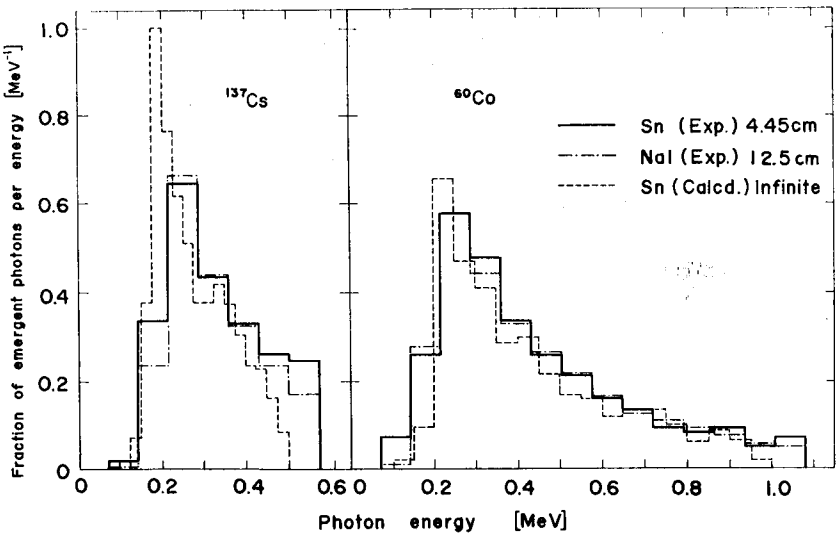

Fig. 7 Energy spectrum of backscattered photons for a 4.45 cm thick tin scatterer. Energy spectrum for a semi-infinite NaI(Tl) scatterer obtained by Nakamura and Hyodo[4], Monte Carlo values[6] for 1.0-MeV and 0.5-MeV gamma rays for a semi-infinite tin scatterer are also shown.

Figure 7 shows the energy spectra $N(E, x)$ at $x=4.45$ cm. They were compared with the energy spectra for semi-infinite tin slab calculated by the Monte Carlo method[6] (1-MeV and 0.5-MeV incident energies). The experimental value is in good agreement with the calculated one for ^{60}Co gamma rays taking the difference of the incident energy into consideration, but for ^{137}Cs gamma rays the calculated value is shifting to the left relative to the experimental value, as the difference of the incident energy is larger than that for ^{60}Co gamma rays. In Fig. 7, the energy spectra for semi-infinite NaI(Tl) scatterer obtained in the previous paper[4] are also shown. They show very good agreement with the experimental values for tin. This also supports the fact that the effective atomic number of NaI is close to tin and that the NaI(Tl) crystal used previously is semi-infinite.

The errors shown in Table I and II are the probable errors based upon the curve fittings by the method of least squares. In addition, there are several unpresumable errors such as the error of the inverse response matrix. Then, as the errors of $\alpha(\infty)$ and $\alpha_E(\infty)$ shown in Table III, we adopted the values of ten times the errors shown in Table II.

References

1) T. Hyodo and S. Shimizu; Bull. Inst. Chem. Research, Kyoto Univ., **39**, 180 (1961)
2) T. Hyodo; Nucl. Sci. Eng., **12**, 178 (1962)

3) H. Fujita, K. Kobayashi and T. Hyodo; Nucl. Sci. Eng., **19**, 437 (1964)
4) T. Nakamura and T. Hyodo; Nuclear Applications, **3**, 446 (1967)
5) K. Mizukami, T. Matsumoto and T. Hyodo; (to be published)
6) M. J. Berger and D. J. Raso; Radiation Research, **12**, 20(1960); Natl. Bur. Standards Report, 5982(1958)
7) A. Shimizu and H. Mizuta; J. Nucl. Sci. Technol., **3**, 57(1966)
8) T. Hyodo and F. Makino; THIS MEMOIRS, **24**, 291 (1962)
9) B. P. Bulatov and E. A. Garusov; Atomnaya Energiya, **5**, 631 (1958), (in Russian)
10) Interpolated values from results of ref. 6 cited in ref. 2